

# Effect of Nutrient Solution Composition on Bio-Cemented Sand

Shihua Liang, Xueli Xiao, Zhanlin Li and Deluan Feng \*

School of Civil and Transportation Engineering, Guangdong University of Technology, Guangdong 510006, China; shihua\_l@gdut.edu.cn (S.L.); 2112009005@mail2.gdut.edu.cn (X.X.); 2112109084@mail2.gdut.edu.cn (Z.L.)

\* Correspondence: wolfluan@126.com

**Abstract:** Microbial-induced carbonate precipitation is an environmentally friendly foundation treatment technology that effectively improves soil engineering performance. The various nutrient components of liquid curing compounds significantly influence the curing effect. On the basis of penetration, dry density, water absorption, and unconfined compressive strength tests, this study showed the effect of nutrient solution composition, including urea, calcium chloride, sodium bicarbonate, ammonium chloride, and nutrient broth, on the physicochemical properties of bio-cemented sand. The morphological differences of calcium carbonate precipitates under nutrient solution composition were compared through scanning electron microscopy (SEM). Results showed that the curing effect of compound nutrient solution was improved compared with the basic nutrient solution (urea and calcium chloride). Among the individual components added, ammonium chloride had the most remarkable effect, followed by sodium bicarbonate and nutrient broth. Among the paired components added, sodium bicarbonate + ammonium chloride had the most significant effect, followed by sodium bicarbonate + nutrient broth and ammonium chloride + nutrient broth. The strength of bio-cemented sand cured with compound nutrient solution containing five components could reach 3.43 MPa, which was 1.92 times higher than the strength of the basic nutrient solution. As shown by the SEM image, the calcium carbonate precipitation in the solidified sand was distributed in the clearance of sand particles, effectively bonding the sand particles. The calcium carbonate obtained by the composition of the compound nutrient solution precipitated the sand particles, and some of the sand particles were wrapped. Moreover, the amount of precipitation was evidently greater than that of the basic nutrient solution. Compared with the basic nutrient solution, the compound nutrient solution effectively reduced the apparent porosity and average pore size of the sand. Thus, the curing effect of the compound nutrient solution was better than that of the basic nutrient solution.



**Citation:** Liang, S.; Xiao, X.; Li, Z.; Feng, D. Effect of Nutrient Solution Composition on Bio-Cemented Sand. *Crystals* **2021**, *11*, 1572. <https://doi.org/10.3390/cryst11121572>

Academic Editor: José L. García

Received: 19 October 2021

Accepted: 14 December 2021

Published: 16 December 2021

**Publisher's Note:** MDPI stays neutral with regard to jurisdictional claims in published maps and institutional affiliations.

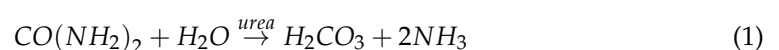


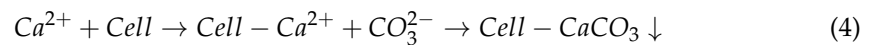
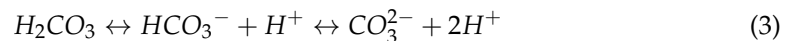
**Copyright:** © 2021 by the authors. Licensee MDPI, Basel, Switzerland. This article is an open access article distributed under the terms and conditions of the Creative Commons Attribution (CC BY) license (<https://creativecommons.org/licenses/by/4.0/>).

**Keywords:** microbial-induced carbonate precipitation; nutrient solution; sand; physicochemical index; SEM

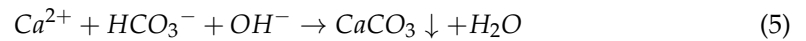
## 1. Introduction

Microbial-induced carbonate precipitation (MICP) is an environmentally friendly soil improvement technology. MICP occurs through calcium carbonate precipitation, which binds sand particles and improves the engineering properties of the soil [1–3], including strength characteristics of improved sand [4–6], and sandy soil liquefaction resistance [7,8]. MICP is also useful in heavy metal repair [9,10] and crack repair [11,12]. The mechanism of action is that the microorganisms themselves metabolize to produce urease during the process of microbial-induced calcium carbonate precipitation, which can hydrolyze urea (Equation (1)). Carbonic acid and ammonia react further after urea is hydrolyzed (Equations (2) and (3)). The cell itself carries a negative charge, calcium ions attach to the cell surface, and microorganisms as nucleation sites bind carbonate ions to form calcium carbonate precipitation (Equation (4)) [13,14].





In addition, the hydrolysis of urea increase the pH of the soil. Calcium and bicarbonate ions form calcium carbonate precipitation under alkaline conditions (Equations (5) and (6)) [15]



Based on the aforementioned reaction, urease-producing microorganisms, urea, and calcium ions are necessary for the reaction to occur. The microorganisms are provided by the bacterial solution, and urea and calcium ions are provided by the nutrient solution. The cementing effect of MICP depends to a great extent on the composition and concentration of cementation solution, which affect not only the crystal type, appearance, size, composition of pore fluid, and pH value [16,17] but also the distribution of bacteria and crystals in the pore spaces [18]. Macroscopically, it affects calcium carbonate production and precipitation efficiency [19]. It also affects the pore size distribution, compression behavior, shear strength, and stiffness of cemented geomaterials. The composition of cementation solution controls the growth and metabolism of microorganisms and the precipitation process of calcium carbonate. More specifically, the composition of cementing cementation affects the activity of bacteria and urease, the type and morphology of calcium carbonate crystal, and the properties of soils. The cementation solution plays an important role in the MICP process. Variations in cementation solution composition can cause different cementing effects [20]. Most basic nutrient solutions are composed of urea and calcium salt [21–23]. However, a compound nutrient solution that includes sodium bicarbonate, ammonium chloride, and nutrient broth can also be added to the nutrient solution [15,24–27]. At present, research on the effect of different components in the compound nutrient solution on the cementation effect and its mechanism is relatively insufficient. In this study, the composition of the nutrient solution was changed in turn, and geotechnical test and scanning electron microscopy (SEM) were performed to observe the changes in order to find the best curing effect of the composition of cementation fluid on MICP solidified sand column and provide reference value for the popularization of MICP in engineering application.

## 2. Materials and Methods

### 2.1. Materials

The primary material was *Sporosarcina ureae* (DSM33), a chemical heterotrophic bacteria that was spherical or ovoid, Gram-positive, and with few flagellar movements. In this experiment, the urease activity of the bacterial liquid was 1.15 mS (cm·min). The culture medium for bacterial expansion was composed of 20 g/L yeast extract, 10 g/L ammonium sulfate, and 2 g/L sodium hydroxide. Fujian (China) ISO standard sand is a fine sand with uniform soil particles and poor gradation. It has a relative density of 2.653 and a porosity of 0.6.

The size of the specimen was 39.1 mm in diameter and 80 mm in height. All tests were triplicated for repeatability. The sample was loaded with a split PVC mold, and standard sand was slowly poured into the mold, layered, and compacted. Two layers of geotextile were used as filters at two ends of the PVC. Each sample was pumped into the bacterial or nutrient solution at a constant rate using a peristaltic pump. Sample preparation required three rounds of circular grouting, and each round of grouting included two processes: bacterial liquid injection and nutrient liquid injection. The first process of each round of grouting was the injection of bacterial liquid. Each sand column was injected with 50 mL of bacterial liquid and 5 mL of 0.05 mol/L calcium chloride solution for each round of grouting. The peristaltic pump controlled the injection speed at 3 mL/min. After injection, the sample was allowed to stand for 2 h. The second process was the injection of nutrient

solution. Each sand column was injected with 50 mL of nutrient solution at a time. The peristaltic pump controlled the injection speed at 3 mL/min. After injection, the sample was allowed to stand for 6–8 h, and the process was repeated nine times to complete a round of grouting.

## 2.2. Test Plan

The compound nutrient solution consists of five main ingredients: calcium chloride, urea, sodium bicarbonate, ammonium chloride, and nutrient broth (10 g/L peptone, 3 g/L beef extract, and 5 g/L sodium chloride). The experimental program is based on the components of the nutrient solution, which are divided into four categories: A, B, C, and D. Category A is the basic group, and Groups B, C, and D represent the control group. The nutrient solution of the basic group only contains calcium chloride and urea. Group B is divided into three categories. On the basis of Group A, sodium bicarbonate, ammonium chloride, and nutrient broth are added, respectively. Group C is divided into three categories. On the basis of Group B, ammonium chloride and nutrient broth, sodium bicarbonate and nutrient broth, and sodium bicarbonate and ammonium chloride are added in two successive combinations. Group D consists of five components: calcium chloride, urea, sodium bicarbonate, ammonium chloride, and nutrient broth. The detailed test plan is shown in Table 1.

**Table 1.** Test plan.

Groups	A	B1	B2	B3	C1	C2	C3	D
CaCl <sub>2</sub> 55 g/L	✓	✓	✓	✓	✓	✓	✓	✓
Urea 30 g/L	✓	✓	✓	✓	✓	✓	✓	✓
NaHCO <sub>3</sub> 2.12 g/L		✓				✓	✓	✓
NH <sub>4</sub> Cl 10 g/L			✓		✓		✓	✓
Nutrient broth 3 g/L				✓	✓	✓		✓

After the MICP treatment, the permeability coefficient, dry density, water absorption, unconfined compressive strength, and calcium carbonate content were measured in sequence. The effect of bio-cemented sand was evaluated through comprehensive analysis of various physical and mechanical parameters, combined with SEM (Carl Zeiss AG, Oberkochen, German) and binary processing of the SEM image by IPP software (IPP 7.0).

## 2.3. Test Methods

**Beaker test:** First, 24 beakers were taken, and their mass  $m_1$  was weighed. Then, 25 mL of the nutrient solutions of A, B, C, and D were poured into the beakers, followed by 25 mL of bacterial solution. The samples were allowed to stand for 24 h until the reaction was completed. Then, the mass  $m_2$  of the beaker and calcium carbonate precipitation was weighed after curing. The calcium carbonate content was  $m_2 - m_1$ . The urease activity was measured after adding different nutrient solutions.

**Permeability coefficient:** Through the variable head penetration test, the initial water height  $h_1$  and the end water height  $h_2$  were determined within a certain period  $\Delta t$ . The permeability coefficient of the sample was calculated according to the following formula:

$$k = 2.3 \frac{al}{A\Delta t} \log \frac{h_1}{h_2} \quad (7)$$

where  $a$  was the cross-sectional area of the water pipe,  $A$  was the cross-sectional area of the sample, and  $l$  was the height of the sample.

**Dry density:** The solidified sand column was dried in a blast drying oven at 80 °C until the mass loss rate within 24 h was less than 0.1%. The dried sand column was cooled at room temperature. Then, its quality, height, and diameter were measured to obtain its dry density.

Water absorption ratio: The mass  $m_1$  of the sand column was measured after drying. Then, the sand column was placed in water for 24 h. The sand column was removed and the excess water on its surface was wiped off. The weight of the sand column was  $m_2$ . The water absorption ratio of the sample was calculated according to the following formula:

$$w = \frac{m_1 - m_2}{m_1} \times 100\% \quad (8)$$

Unconfined compressive strength: After the bio-solidified sample was dried for 24 h, it was placed on the testing machine so that the sample and the upper and lower loading plates of the testing machine were in contact. Thereafter, the force was cleared, and the test was started. The test loading rate was set to 1 mm/min, and the unconfined compressive strength value was recorded after the sample was broken.

Secant modulus E50: Considering that the stress–strain curve of microbial solidified sand materials is similar to the mechanical characteristics of sandstone, the secant modulus E50 in rock mechanics was used to represent the elastic modulus of microbial solidified sand. The secant modulus E50 is the ratio of the stress value to the strain value corresponding to half of the peak stress in the stress–strain curve.

Calcium carbonate content: The broken sand block is placed in a beaker, and its mass WS1 is weighed. The mass of the selected sand blocks for each group was approximately 40 g to ensure the accuracy of the test results (Figure 1). The sand block was soaked in 5 mol/L concentrated hydrochloric acid solution. Calcium carbonate is considered to be completely dissolved when no air bubbles are generated. The completely reacted sand sample is rinsed with deionized water and placed in an oven for drying. The mass of the beaker and sand sample is called WS2. The calcium carbonate content of the sample is calculated according to Formula (9) [28,29].

$$C_{CaCO_3} = \frac{w_{s1} - w_{s2}}{w_{s2}} \times 100\% \quad (9)$$

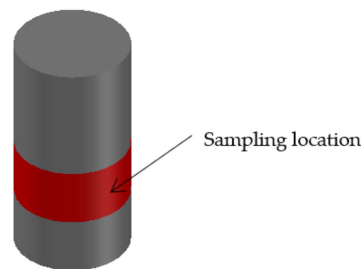


Figure 1. Sample.

SEM test: The dried sample is placed on the sample holder for gold spray pretreatment. Then, the sample is scanned, and a picture with a magnification of 1000 on the screen is taken. IPP software is used for binary processing of the SEM image [30–32].

### 3. Results

#### 3.1. Beaker Test

According to the composition of the nutrient solution, the content of calcium carbonate produced is added to the beaker with bacterial liquid and various nutrient solutions as shown in Figure 2a. Among the four types of nutrient solutions (A, B, C, and D), the average calcium carbonate content of the compound nutrient solution of Group D was the highest, and the average calcium carbonate content of the basic nutrient solution of Group A was the lowest. In the Group B test, the average calcium carbonate content only added with ammonium chloride was the highest. In the Group C test, the average calcium carbonate content added with sodium bicarbonate + ammonium chloride was the highest.

These findings showed that the compound nutrient solution could effectively promote the production of calcium carbonate. Figure 2b shows that the addition of the nutrient complex increased the urease activity.

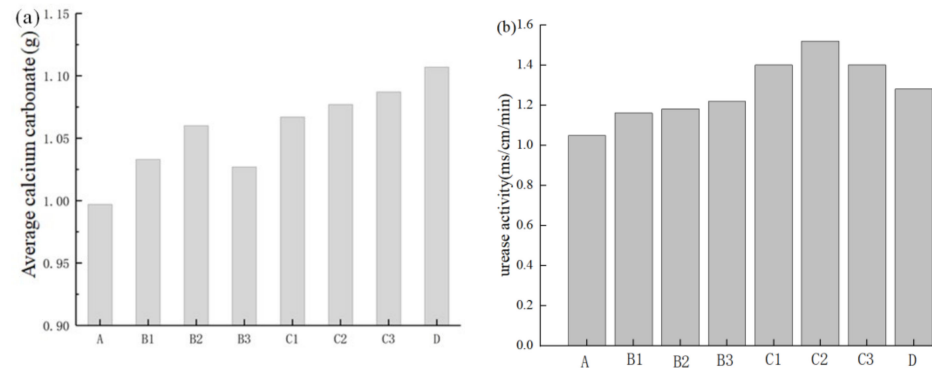


**Figure 2.** Average calcium carbonate content (a) and urease activity (b).

### 3.2. Geotechnical Test

Geotechnical tests were conducted on the solidified sand samples (Figure 3). Compared with the basic nutrient solution, the compound nutrient solution after sodium bicarbonate, ammonium chloride, and nutrient broth were arbitrarily added could effectively reduce the permeability coefficient and water absorption rate of the sand column after solidification. The dry density, unconfined compressive strength, calcium carbonate content, and secant modulus E50 were effectively improved, indicating that the solidification effect of the compound nutrient solution was significantly better than that of the basic nutrient solution.

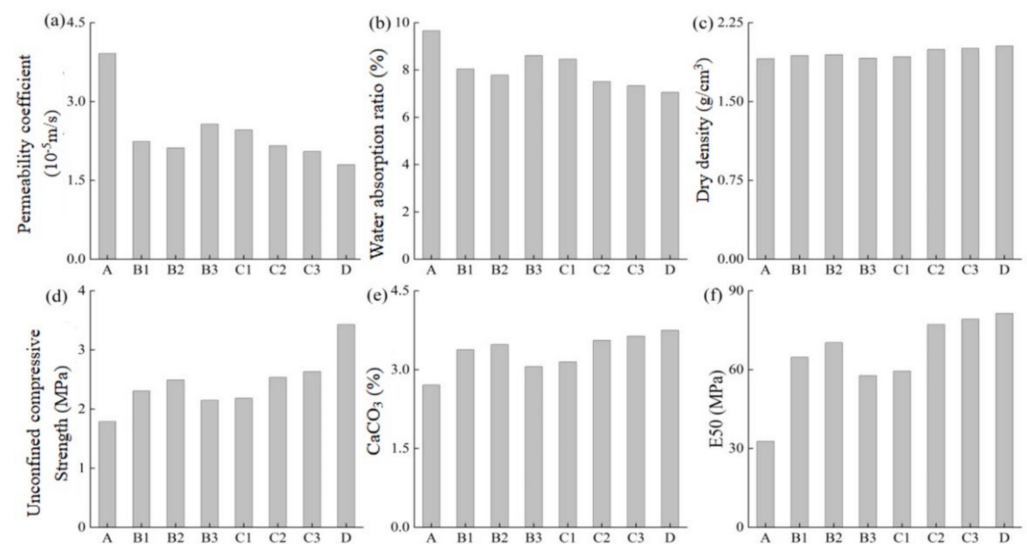


**Figure 3.** Physical and mechanical indicators of sand solidified with various nutrient solution compositions. Permeability coefficient (a); water absorption ratio (b); dry density (c); unconfined compressive strength (d);  $\text{CaCO}_3$  (e); E50 (f).

For Group B, in which sodium bicarbonate, ammonium chloride, and nutrient broth were added, only adding ammonium chloride had the lowest permeability coefficient and water absorption, followed by sodium bicarbonate and nutrient broth. Only adding ammonium chloride had the highest dry density, unconfined compressive strength, calcium carbonate content, and secant modulus E50, followed by sodium bicarbonate and nutrient broth.

For Group C with two kinds of sodium bicarbonate, ammonium chloride, and nutrient broth, the compound nutrient solution of sodium bicarbonate + ammonium chloride had the lowest permeability coefficient and water absorption rate, followed by sodium bicarbonate + nutrient broth and ammonium chloride + nutrient broth. The compound nutrient solution of sodium bicarbonate + ammonium chloride had the highest dry density, unconfined compressive strength, calcium carbonate content, and secant modulus E50, followed by sodium bicarbonate + nutrient broth and ammonium chloride + nutrient broth.

The sand column solidified by the compound nutrient solution of Group D had the best solidification effect. Its permeability coefficient, water absorption rate, dry density, unconfined compressive strength, calcium carbonate content, and secant modulus E50 were  $1.8 \times 10^{-5}$  m/s, 7.06%, 2.029 g/cm<sup>3</sup>, 3.43 MPa, 3.75%, and 81.414 MPa, respectively. Compared with the basic nutrient solution, the permeability coefficient and water absorption rate were reduced by 53.96% and 26.92%, respectively. The dry density, unconfined compressive strength, calcium carbonate content, and secant modulus E50 were increased by 6.34%, 91.94%, 38.33%, and 148.55%, respectively.

The stress–strain curves of the sand samples solidified with different nutrient solution compositions are shown in Figure 4. Regardless of whether the basic nutrient or the compound nutrient solution was used, the stress–strain curve of the sand column after solidification showed a similar trend. Before the peak stress was reached, the stress increased with the increase of strain. The growth rate of the compound nutrient solution solidified sand column was greater than that of the basic nutrient solution. After reaching the peak, the strain continued to increase, whereas the stress gradually decreased, and the column exhibited typical brittle failure characteristics.

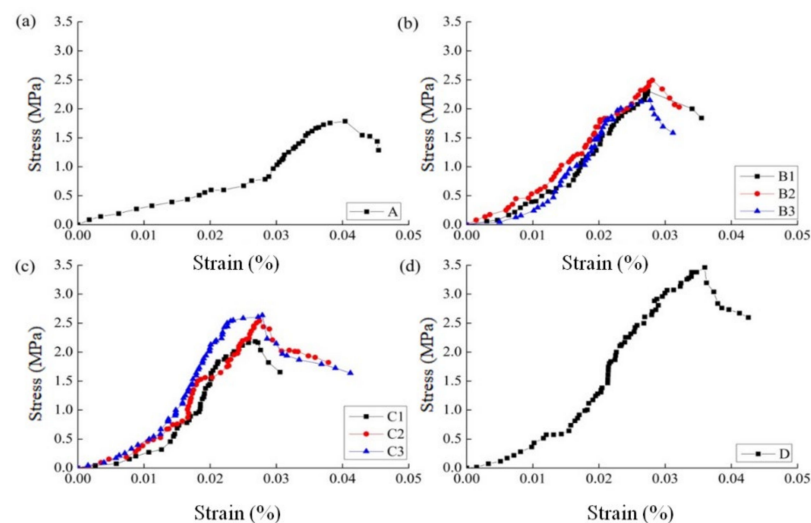


**Figure 4.** Stress–strain curve of sand solidified with various nutrient solution compositions. Stress–strain of group A (a); Stress–strain of group B (b); Stress–strain of group C (c); Stress–strain of group D (d).

### 3.3. SEM

The solidified sand column with various nutrient solution components was analyzed by SEM after drying, and the connections of sand particles were magnified 1000 times. Figure 5 shows that the basic nutrient and compound nutrient solutions can produce calcium carbonate precipitation at the contact parts of the sand particles and effectively bind them, thereby improving the unconfined compressive strength. The calcium carbonate precipitation produced by Group A was very limited, and those produced by Groups B, C, and D were greater. Among them, Group D produced the highest level of precipitation, followed by Groups C and B. Sodium bicarbonate, ammonium chloride, and nutrient broth all promote microbial-induced calcium carbonate precipitation. However, one component

was added in Group B, two components in Group C, and all components in Group D. Thus, Group D produced the most precipitation, and its strength reached 3.43 MPa. The calcium carbonate precipitates generated in Group D not only bound the sand particles but also gradually wrapped part of the sand particles, effectively enhancing the connection strength between the soil particles.

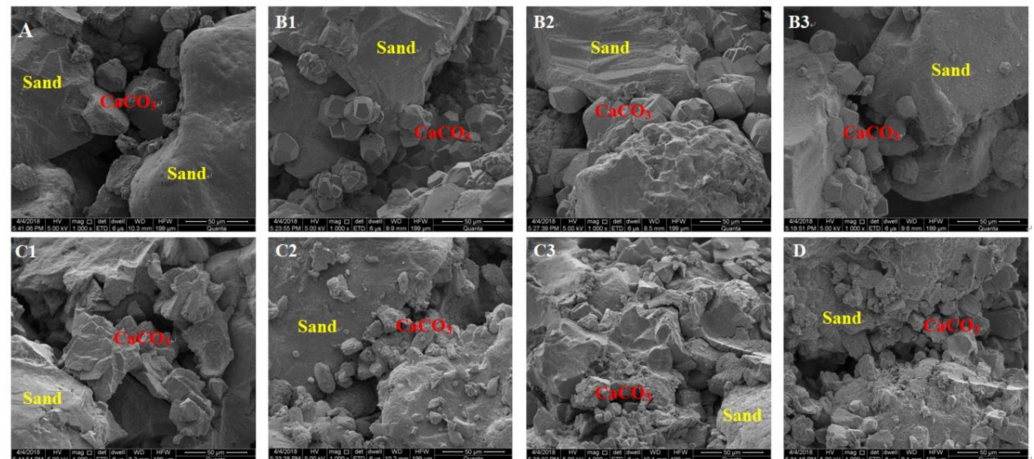


**Figure 5.** SEM image of sand solidified with various nutrient solution compositions. SEM image of group A (A); SEM image of group B1 (B1); SEM image of group B2 (B2); SEM image of group B3 (B3); SEM image of group C1 (C1); SEM image of group C2 (C2); SEM image of group C3 (C3); SEM image of group D (D).

IPP software was used for the binary processing of SEM images of solidified sand with various nutrient solution components (Figure 6). The quantitative analysis according to binarization pictures, statistics of microscopic pore distribution, calculation of apparent porosity, and average pore size were conducted (Figure 7 and Table 2).

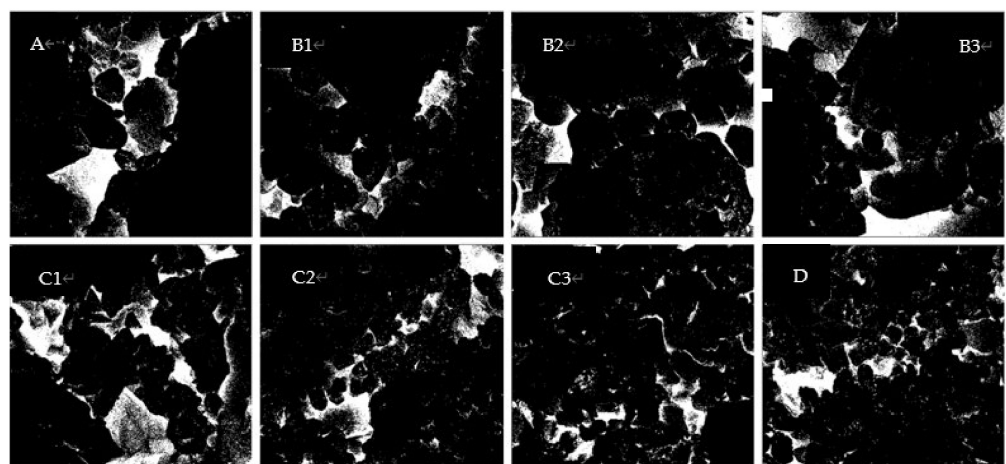


**Figure 6.** SEM images of sand solidified with various nutrient solution compositions. SEM image of group A (A); SEM image of group B1 (B1); SEM image of group B2 (B2); SEM image of group B3 (B3); SEM image of group C1 (C1); SEM image of group C2 (C2); SEM image of group C3 (C3); SEM image of group D (D).

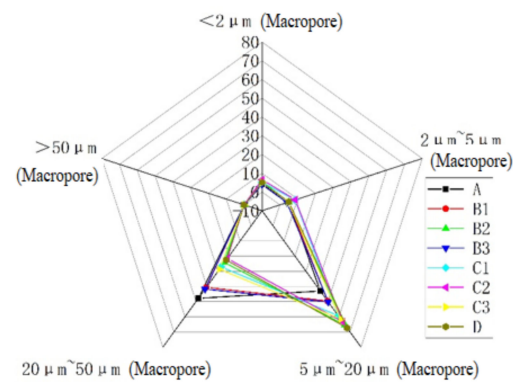


**Figure 7.** Radar map of pore size distribution of solidified sand column with different nutrient solutions.

**Table 2.** Statistical analysis of microstructure pore size distribution of sand solidified with different nutrient solution compositions.

Sample	Percentage of Various Pores ( $\mu\text{m}$ )					Apparent Porosity	Average Pore Diameter
	<2	2~5	5–20	20–50	>50	%	$\mu\text{m}$
A	4.15	5.03	42.97	47.85	0.00	17.50	42.83
B1	4.91	4.90	49.60	40.59	0.00	10.15	26.45
B2	5.46	4.98	65.39	24.18	0.00	8.99	22.59
B3	3.90	4.04	50.29	41.76	0.00	11.98	33.60
C1	5.18	8.50	59.18	27.14	0.00	10.25	28.47
C2	6.50	8.68	63.26	21.57	0.00	7.88	19.99
C3	4.99	4.80	61.58	28.63	0.00	5.90	15.42
D	5.08	5.04	67.34	22.54	0.00	3.54	10.52

The various pore sizes of solidified sands with different nutrient solution components are divided into five categories: hole ( $>50 \mu\text{m}$ ), macropore ( $20\text{--}50 \mu\text{m}$ ), mesopore ( $5\text{--}20 \mu\text{m}$ ), small pore ( $2\text{--}5 \mu\text{m}$ ), and micropore ( $<2 \mu\text{m}$ ) [33]. As shown in Table 2 and Figure 7, the microscopic pores of sands solidified with various nutrient solution components have no holes. The proportion of macropores and mesopores is relatively large, and that of small pores and micropores is relatively small. A comparison of the unconfined compressive strength (Figure 4) shows that the curing strength gradually increases, the proportion of mesopores in the sand column gradually increases, and the proportion of macropores gradually decreases from Group A to Group D. As shown in Figure 5, the increase in curing strength may be due to the increase in calcium carbonate content, which caused some large pores to be filled and transformed into mesopores.

Figures 6 and 8 show that Group A had the highest apparent porosity and average pore size. After 1–3 kinds of sodium bicarbonate, ammonium chloride, and nutrient broth were added, the apparent porosity and average pore diameter of the sand column were reduced, with Group D showing the greatest decrease, followed by Groups C and B. The apparent porosity and average pore size of the sand solidified by the compound nutrient solution added with five components reached 3.54% and  $10.52 \mu\text{m}$ , which were reduced by 79.77% and 75.44% compared with the basic nutrient solution, respectively.

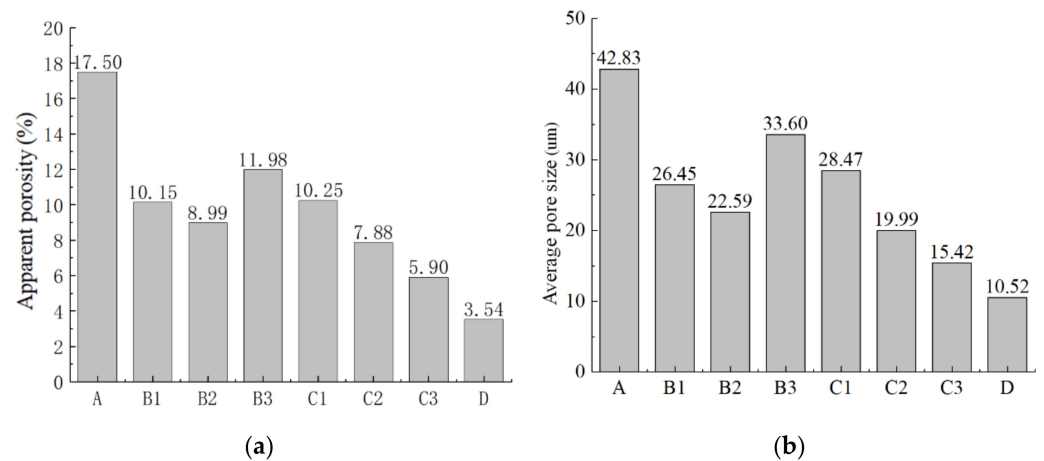


**Figure 8.** Quantitative analysis of SEM images of sand solidified with various nutrient solution compositions. (a) Apparent porosity; (b) average pore size.

After solidification of the various nutrient solution components, the sand sample was analyzed by SEM at  $2000\times$  magnification (Figure 9). The difference in the composition of the nutrient solution affected not only the amount of calcium carbonate precipitation but also the calcium carbonate crystal form. The calcium carbonate precipitates of Group A showed prismatic crystals, and calcium carbonate particles were scattered in the sand column. The calcium carbonate precipitates in Groups B, C, and D showed clusters of interlaced particles. A comparison of Groups B and C show that the surface of calcium carbonate precipitated crystals produced by the nutrient solution without nutrient broth was relatively smooth. When the nutrient broth was added in the nutrient solution, the surface of calcium carbonate precipitates was relatively rough and accompanied by fine pores. The solidification effect was improved when 1–3 kinds of sodium bicarbonate, ammonium bicarbonate, and nutrient broth were added to the nutrient solution to form a compound nutrient solution. The calcium carbonate precipitates produced in Groups B, C, and D presented stacked clusters with more content than Group A and Group D having the greatest content.

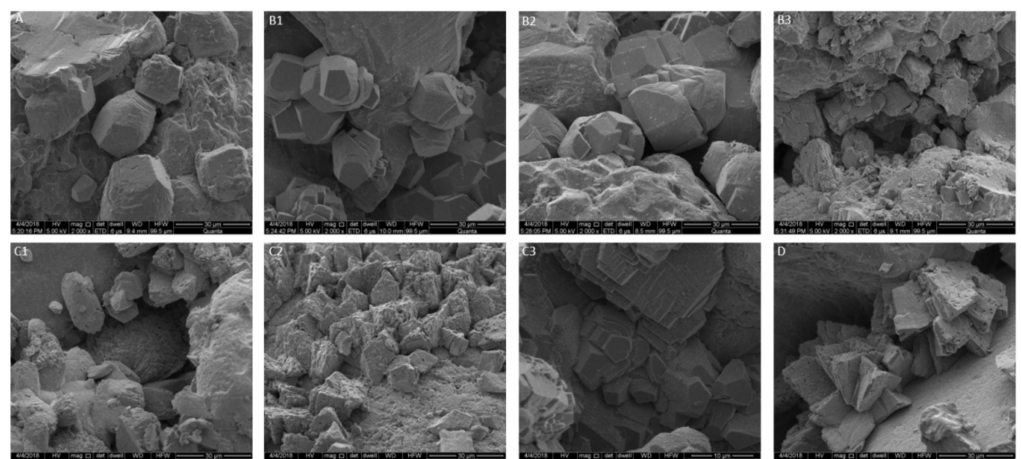


**Figure 9.** Calcium carbonate crystal form of sand solidified with various nutrient solutions. Calcium carbonate crystal form of group A (A); Calcium carbonate crystal form of group B1 (B1); Calcium carbonate crystal form of group B2 (B2); Calcium carbonate crystal form of group B3 (B3); Calcium carbonate crystal form of group C1 (C1); Calcium carbonate crystal form of group C2 (C2); Calcium carbonate crystal form of group C3 (C3); Calcium carbonate crystal form of group D (D).

### 3.4. Influence Mechanism of Various Nutrient Solution Components

The test results showed that the compound nutrient solution enhances the sand solidification effect more effectively than the basic nutrient solution does. Among the compound nutrient solutions with one ingredient added, ammonium chloride had the best lifting effect, followed by sodium bicarbonate and nutrient broth.

The reason is that, from the perspective of reaction balance, the addition of sodium bicarbonate promotes the hydrolysis of bicarbonate radicals. By enhancing the reaction Formula (10), the generated carbonate ions increase, thereby promoting the generation of calcium carbonate precipitation and increasing the curing effect [34,35]. The addition of ammonium chloride promotes the reaction Formula (11) [35,36]. The ammonium ion combines with the hydroxide ion to form ammonia gas and water. The addition of nutrient broth can provide microorganisms with nutrients and promote their growth as well as the formation of microbial-induced calcium carbonate precipitation. The addition of sodium bicarbonate and ammonium chloride mainly affects chemical reactions, whereas the addition of nutrient broth mainly affects microorganisms. Microorganism-induced calcium carbonate precipitation involves not only microorganisms but also related chemical reactions. Therefore, ammonium chloride, sodium bicarbonate, and nutrient broth have a mutual influence in promoting microbe-induced calcium carbonate precipitation. The best solidification effect occurs when ammonium chloride, sodium bicarbonate, and nutrient broth are added to the nutrient solution at the same time. However, these compounds have various promotion effects on the solidification effect, and the mechanism behind their effects remains to be further explored.

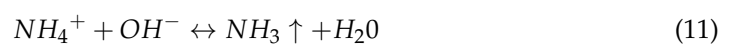
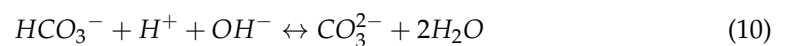


Figure 3 shows that the stress of Groups B, C, and D increases with strain significantly faster than that of Group A. The addition of sodium bicarbonate, ammonium chloride, and nutrient broth effectively promotes the formation of calcium carbonate precipitation and improves the strength and rigidity of the sand column. In the SEM images (Figures 4 and 5), the number of calcium carbonate deposits used to bond the sand particles generated in Groups B, C, and D were greater than those in Group A.

## 4. Conclusions

Through the comparative analysis of the composition of the compound nutrient solution, we obtained several conclusions. The addition of sodium bicarbonate, ammonium chloride, and nutrient broth in the compound nutrient solution could effectively improve the curing effect. For the compound nutrient solution added with one ingredient, ammonium chloride had the best lifting effect. For the compound nutrient solution with two ingredients added, sodium bicarbonate and nutrient broth had the best lifting effect. For the compound nutrient solution that contained components including sodium bicarbonate, chloride, and nutrient broth, the lifting effect was better than that of either adding with one or two components of the compound nutrient solution. The strength of bio-cemented sand cured with the compound nutrient solution containing five components could reach 3.43 MPa, which was 1.92 times higher than the strength of the basic nutrient solution. In the SEM image, the calcium carbonate precipitates generated by the bio-solidified sand were distributed in the interstices of the sand particles, effectively binding the sand particles to increase the strength. Moreover, the calcium carbonate content of the sand solidified with compound nutrient solution was significantly higher than that of the basic nutrient solution. The results of SEM image binarization showed that the compound nutrient solution could effectively reduce the apparent porosity and average pore size of the sand compared with the basic nutrient solution, and its curing effect was better than that of the latter.

**Author Contributions:** Conceptualization, S.L.; writing, D.F.; formal analysis, D.F.; data curation, X.X.; supervision, Z.L. All authors have read and agreed to the published version of the manuscript.

**Funding:** This study was funded by the National Natural Science Foundation of China (Grant No. 52078142) and the Science and Technology Program of Guangzhou, China (Grant No. 202002030194).

**Data Availability Statement:** The data used to support the findings of this study are included within the article.

**Conflicts of Interest:** The authors declare no conflict of interest.

## References

1. Liu, P.; Shao, G.; Huang, R. Study of the interactions between *S. pasteurii* and indigenous bacteria and the effect of these interactions on the MICP. *Arab. J. Geosci.* **2019**, *12*, 1–10. [[CrossRef](#)]
2. Wang, X.M.; Guo, W.; Yu, F. Experimental study of effect of nutrient concentration on physico-mechanical properties of cemented sand. *Rock Soil Mech.* **2016**, *37*, 363–368.
3. Li, Y.; Guo, Z.; Wang, L.; Li, Y.; Liu, Z. Shear Resistance of MICP Cementing Material at the Interface between Calcareous Sand and Steel. *Mater. Lett.* **2020**, *274*, 128009. [[CrossRef](#)]
4. Liu, S.; Wen, K.; Amini, F.; Li, L. Investigation of Nonwoven Geotextiles for Full Contact Flexible Mould Used in Preparation of MICP-treated Geomaterial. *Int. J. Geosynth. Ground Eng.* **2020**, *6*, 1–12. [[CrossRef](#)]
5. Imran, A.; Gowthaman, S.; Nakashima, K.; Kawasaki, S. The Influence of the Addition of Plant-Based Natural Fibers (Jute) on Biocemented Sand Using MICP Method. *Materials* **2020**, *13*, 4198. [[CrossRef](#)]
6. Liu, K.W.; Jiang, N.J.; Qin, J.D.; Wang, Y.J.; Tang, C.S.; Han, X.L. An experimental study of mitigating coastal sand dune erosion by microbial- and enzymatic-induced carbonate precipitation. *Acta Geotech.* **2021**, *16*, 467–480. [[CrossRef](#)]
7. Zhang, X.; Chen, Y.; Liu, H.; Zhang, Z.; Ding, X. Performance evaluation of a MICP-treated calcareous sandy foundation using shake table tests. *Soil Dyn. Earthq. Eng.* **2020**, *129*, 105959. [[CrossRef](#)]
8. Xiao, P.; Liu, H.; Stuedlein, A.; Evans, T.M.; Xiao, Y. Effect of relative density and biocementation on cyclic response of calcareous sand. *Can. Geotech. J.* **2019**, *56*, 1849–1862. [[CrossRef](#)]
9. Qiao, S.; Zeng, G.; Wang, X.; Dai, C.; Sheng, M.; Chen, Q.; Xu, F.; Xu, H. Multiple heavy metals immobilization based on microbially induced carbonate precipitation by ureolytic bacteria and the precipitation patterns exploration. *Chemosphere* **2021**, *274*, 129661. [[CrossRef](#)] [[PubMed](#)]
10. He, J.; Chen, X.; Zhang, Q.; Achal, V. More effective immobilization of divalent lead than hexavalent chromium through carbonate mineralization by *Staphylococcus epidermidis* HJ2—ScienceDirect. *Int. Biodeterior. Biodegrad.* **2019**, *140*, 67–71. [[CrossRef](#)]
11. Liu, S.; Yu, J.; Peng, X.; Cai, Y.; Tu, B. Preliminary study on repairing tabia cracks by using microbially induced carbonate precipitation. *Constr. Build. Mater.* **2020**, *248*, 1–12. [[CrossRef](#)]
12. Sun, X.; Miao, L.; Wu, L.; Wang, H. Theoretical quantification for cracks repair based on microbially induced carbonate precipitation (MICP) method. *Cem. Concr. Compos.* **2021**, *118*, 103950. [[CrossRef](#)]
13. Xing, G.; Jiuge, N.; Shihua, L.; Deluan, F.; Qingzi, L. Environmental effect of grouting batches on Microbial-Induced Calcite Precipitation. *Ekoloji* **2019**, *28*, 929–936.
14. Arpajitrakul, S.; Pungrasmi, W.; Likitlersuang, S. Efficiency of microbially-induced calcite precipitation in natural clays for ground improvement. *Constr. Build. Mater.* **2021**, *282*, 122722. [[CrossRef](#)]
15. Dejong, J.T.; Fritzges, M.B.; Nüsslein, K. Microbially Induced Cementation to Control Sand Response to Undrained Shear. *J. Geotech. Geoenviron. Eng.* **2006**, *132*, 1381–1392. [[CrossRef](#)]
16. McWhirter, M.J.; McQuillan, A.J.; Bremer, P.J. Influence of ionic strength and pH on the first 60 min of *Pseudomonas aeruginosa* attachment to ZnSe and to TiO<sub>2</sub> monitored by ATR-IR spectroscopy. *Colloids Surf. B-Biointerfaces* **2002**, *26*, 365–372. [[CrossRef](#)]
17. Harkes, M.P.; van Paassen, L.A.; Booster, J.L.; Whiffin, V.S.; van Loosdrecht, M.C.M. Fixation and distribution of bacterial activity in sand to induce carbonate precipitation for ground reinforcement. *Ecol. Eng.* **2010**, *36*, 112–117. [[CrossRef](#)]
18. Stocks-Fischer, S.; Galinat, J.K.; Bang, S.S. Microbiological precipitation of CaCO<sub>3</sub>. *Soil Biol. Biochem.* **1999**, *31*, 1563–1571. [[CrossRef](#)]
19. Cussac, V.; Ferrero, R.L.; Labigne, A. Expression of *Helicobacter pylori* urease genes in *Escherichia coli* grown under nitrogen-limiting conditions. *J. Bacteriol.* **1992**, *174*, 2466–2473. [[CrossRef](#)]
20. Tang, C.-S.; Yin, L.-Y.; Jiang, N.-J.; Zhu, C.; Zeng, H.; Li, H.; Shi, B. Factors affecting the performance of microbial-induced carbonate precipitation (MICP) treated soil: A review. *Environ. Earth Sci.* **2020**, *79*, 1–23. [[CrossRef](#)]
21. Zhang, Y.; Guo, H.; Cheng, X. Role of calcium sources in the strength and microstructure of microbial mortar. *Constr. Build. Mater.* **2015**, *77*, 160–167. [[CrossRef](#)]
22. Cui, M.-J.; Zheng, J.-J.; Zhang, R.-J.; Lai, H.-J.; Zhang, J. Influence of cementation level on the strength behaviour of bio-cemented sand. *Acta Geotech.* **2017**, *12*, 971–986. [[CrossRef](#)]
23. Yang, Z.; Cheng, X. A performance study of high-strength microbial mortar produced by low pressure grouting for the reinforcement of deteriorated masonry structures. *Constr. Build. Mater.* **2013**, *41*, 505–515. [[CrossRef](#)]

24. Zhao, Q.; Li, L.; Li, C.; Li, M.; Amini, F.; Zhang, H. Factors Affecting Improvement of Engineering Properties of MICP-Treated Soil Catalyzed by Bacteria and Urease. *J. Mater. Civ. Eng.* **2014**, *26*, 04014094. [[CrossRef](#)]
25. Li, M.; Li, L.; Ogbonnaya, U.; Wen, K.; Tian, A.; Amini, F. Influence of Fiber Addition on Mechanical Properties of MICP-Treated Sand. *J. Mater. Civ. Eng.* **2016**, *28*, 04015166. [[CrossRef](#)]
26. Li, C.; Yao, D.; Liu, S.; Zhou, T.; Bai, S.; Gao, Y.; Li, L. Improvement of Geomechanical Properties of Bio-remediated Aeolian Sand. *Geomicrobiol. J.* **2018**, *35*, 132–140. [[CrossRef](#)]
27. Mortensen, B.M.; Haber, M.J.; DeJong, J.T.; Caslake, L.F.; Nelson, D.C. Effects of environmental factors on microbial induced calcium carbonate precipitation. *J. Appl. Microbiol.* **2011**, *111*, 338–349. [[CrossRef](#)] [[PubMed](#)]
28. Lin, H.; Suleiman, M.T.; Brown, D.G.; Kavazanjian, E., Jr. Mechanical Behavior of Sands Treated by Microbially Induced Carbonate Precipitation. *J. Geotech. Geoenviron. Eng.* **2016**, *142*, 04015066. [[CrossRef](#)]
29. Whiffin, V.S.; van Paassen, L.A.; Harkes, M.P. Microbial carbonate precipitation as a soil improvement technique. *Geomicrobiol. J.* **2007**, *24*, 417–423. [[CrossRef](#)]
30. Jiang, N.-J.; Soga, K.; Kuo, M. Microbially Induced Carbonate Precipitation for Seepage-Induced Internal Erosion Control in Sand-Clay Mixtures. *J. Geotech. Geoenviron. Eng.* **2017**, *143*, 04016100. [[CrossRef](#)]
31. Dai, C.-X.; Zhang, Q.-F.; He, S.-H.; Zhang, A.; Shan, H.-F.; Xia, T.-D. Variation in Micro-Pores during Dynamic Consolidation and Compression of Soft Marine Soil. *J. Mar. Sci. Eng.* **2021**, *9*, 750. [[CrossRef](#)]
32. Han, P.-j.; Wang, S.; Chen, F.Y.; Bai, X.-h. Mechanism of cement-stabilized soil polluted by magnesium sulfate. *J. Cent. South Univ.* **2015**, *22*, 1869–1877. [[CrossRef](#)]
33. Gong, X.; Niu, J.; Liang, S.; Feng, D.; Luo, Q. Solidification of Nansha soft clay using cement-based composite curing agents. *Adv. Cem. Res.* **2020**, *32*, 66–77. [[CrossRef](#)]
34. Al Qabany, A.; Soga, K. Effect of chemical treatment used in MICP on engineering properties of cemented soils. *Geotechnique* **2013**, *63*, 331–339. [[CrossRef](#)]
35. Anbu, P.; Kang, C.-H.; Shin, Y.-J.; So, J.-S. Formations of calcium carbonate minerals by bacteria and its multiple applications. *Springerplus* **2016**, *5*, 1–26. [[CrossRef](#)] [[PubMed](#)]
36. Chuo, S.C.; Mohamed, S.F.; Setapar, S.H.M.; Ahmad, A.; Jawaid, M.; Wani, W.A.; Yaqoob, A.A.; Ibrahim, M.N.M. Insights into the Current Trends in the Utilization of Bacteria for Microbially Induced Calcium Carbonate Precipitation. *Materials* **2020**, *13*, 4993. [[CrossRef](#)]